ACS APPLIED MATERIALS & INTERFACES

www.acsami.org

Research Article

Chemoenzymatic Cascade Reaction for Green Cleaning of Polyamide Nanofiltration Membrane

Jinxuan Zhang,[‖] Huiru Zhang,[‖] Yinhua Wan, and Jianquan Luo*

Cite This: https://doi.org/10.1021/acsami.1c23466

Read Online

ACCESS | Metrics & More | Article Recommendations | Supporting Information

ABSTRACT: Chemical cleaning is indispensable for the sustainable operation of nanofiltration (NF) in wastewater treatment. However, the common chemical cleaning methods are plagued by low cleaning efficiency, high chemical consumption, and separation performance deterioration. In this work, a chemoenzymatic cascade reaction is proposed for pollutant degradation and polyamide NF membrane cleaning. Glucose oxidase (GOD) enzymatic reaction in this cascade system produces hydrogen peroxide (H_2O_2) and gluconic acid to trigger the oxidation of foulants by Fe_3O_4-catalyzed Fenton reaction. By virtue of the microenvironment (pH and H_2O_2 concentration) engineering and substrate enrichments, this chemoenzymatic cascade reaction (GOD−Fe_3O_4) exhibits a favorable degradation efficiency for bisphenol A and methyl blue (MB). Thanks to the strong oxidizing degradation, the water flux of the NF10 membrane fouled by MB is almost completely recovered (~95.8%) after a 3-cycle fouling/cleaning experiment. Meanwhile, the chemoenzymatic cascade reaction improves the applicability of the Fenton reaction in polyamide NF membrane cleaning because it prevents the membrane from damaging by high concentration of H_2O_2 and inhibits the secondary fouling caused by ferric hydroxide precipitates. By immobilizing GOD on the aminated Fe_3O_4 nanoparticles, a reusable cleaning agent is prepared for highly efficient membrane cleaning. This chemoenzymatic cascade reaction without the addition of an acid/base/oxidant provides a promising candidate for sustainable and cost-effective cleaning for the polyamide NF membrane.

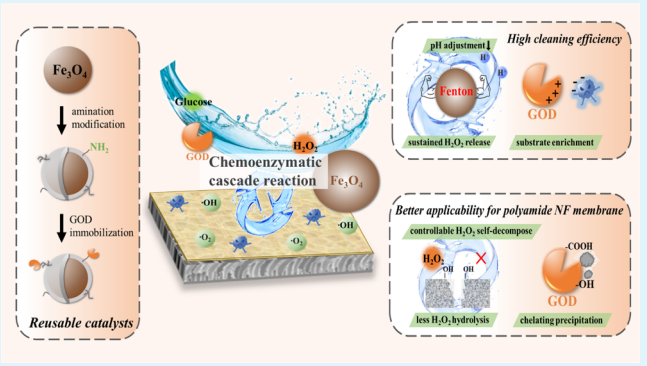

KEYWORDS: *hydrogen peroxide, Fenton reaction, chemoenzymatic cascade reaction, membrane fouling, membrane cleaning*

1. INTRODUCTION

The nanofiltration (NF) membrane technology is one of the widely used membrane processes for wastewater treatment due to its high separation efficiency and low energy consumption.[1−4] During the separation process, membrane fouling inevitably occurs as foulants deposit on/into the membrane, resulting in the reduction of membrane perm-selectivity and impeding the continuous operation of the NF process. Chemical cleaning, such as acid, alkali, and oxidant cleaning, is a routine strategy to deal with industrial membrane fouling problems and restore the membrane performance.[5,6] However, acid cleaning and alkali cleaning are insufficient for completely removing stubborn fouling and have the disadvantage of high chemical consumption. For example, Wang et al. found that NaOH and HCl exhibited low cleaning efficiency of less than 15% on the fouled membrane after a long-term wastewater treatment.[7] Moreover, membrane swelling resulting from the alkaline cleaning would render the temporary enlargement of the membrane pores, reducing solute rejection and causing severe pore blocking. Huang et al. claimed that the swelling of the NF membrane after alkaline cleaning resulted in a significant increase in irreversible pore fouling, and the alkaline cleaning efficiency for the NF membrane was decaying in subsequent fouling/cleaning cycles.[8] Oxidant cleaning can destroy the stubborn fouling layer by degrading organic foulants but has a risk of damaging the NF membrane matrix materials.[9] Specifically, sodium hypochlorite is a commonly used oxidant in industrial membrane cleaning, but most commercially available NF membranes possess a polyamide separation layer with low chlorine tolerance. Besides, sodium hypochlorite cleaning is not an eco-friendly option because of the high chlorine dose and toxic byproducts. By contrast, H_2O_2 is a milder oxidant and therefore less damaging to the polyamide separation layer than sodium hypochlorite.[10] Moreover, it is considered to be a green alternative because oxygen and water are the only products of its decomposition.

Received: December 4, 2021
Accepted: February 2, 2022

However, the membrane cleaning efficiency of H_2O_2 is not always satisfactory due to its low decomposition rate.[11]

Fenton reaction can be utilized to accelerate the decomposition of H_2O_2 through the oxidation of ferric ions (Formula 1 and 2) and produce hydroxyl radicals, which are non-selective oxidants and have stronger oxidation ability than H_2O_2.[12] To date, Fenton reaction has been widely used for the degradation of organic components in wastewater treatment due to its remarkable oxidation capability and having potential in the application of high-effective NF membrane cleaning.[13−15] However, the Fenton cleaning strategy has some intrinsic shortcomings in the cleaning of the polyamide NF membrane. On the one hand, the Fenton reaction requires an acidic environment to ensure the stable Fe^{2+}/Fe^{3+} transformation and avoid the precipitation of ferric hydroxide, and H_2O_2 has greater stability under acidic conditions.[16] The massive consumption of acidic reagents is environmentally hazardous and increases the chemical waste treatment cost. On the other hand, the transportation and storage of H_2O_2 is costly and of great risk.[17] Directly adding high concentration of H_2O_2 in the Fenton cleaning system would also impair the polyamide separation layer.

$$Fe^{2+} + H_2O_2 \rightarrow Fe^{3+} + OH\cdot \quad (1)$$

$$OH\cdot + \text{organic pollutants} \rightarrow \text{oxidation products} \quad (2)$$

To address the above problems, herein, a chemoenzymatic cascade reaction using glucose oxidase (GOD) and Fe_3O_4 nanoparticles as catalysts was proposed for foulant degradation and polyamide NF membrane cleaning. Specifically, GOD enzymatic reaction was initiated by glucose, and the generated gluconic acid would decrease the pH of the system, which was supposed to improve the Fe_3O_4-catalyzed Fenton reaction with the produced H_2O_2.[18,19] The advantages of such a chemoenzymatic cascade reaction over the single enzymatic/Fenton reaction in BPA and MB degradation have been explored. The efficiency and reusability of the cascade reaction for polyamide NF membrane cleaning and its effect on membrane performance were investigated. Thanks to the in-situ production of H_2O_2 in this chemoenzymatic cascade reaction, the risk of membrane damage has been effectively reduced compared to the direct addition of H_2O_2 with high concentration in the traditional Fenton reaction.

For the purpose of cost-efficiency and sustainability, we further designed a reusable catalyst (GOD@Fe_3O_4), which can be recovered under an external magnetic field by amination modification and GOD immobilization on Fe_3O_4 nanoparticles. This study not only proposes a highly efficient and sustainable method for the fouling removal of the polyamide NF membrane without the addition of an acid/base/oxidant but also provides a feasible approach to optimize Fenton cleaning, thus offering guidance for the design of a green cleaning strategy for the NF membrane.

2. EXPERIMENTAL SECTION

2.1. Materials and Chemicals. The chemical catalyst Fe_3O_4 nanoparticle and the biological catalyst GOD for the chemoenzymatic cascade reaction were supplied by Macklin Biochemical Co. and Sigma-Aldrich, respectively. Two commercially available polyamide NF membranes (NF5 and NF10) were used in this work. They have molecular weight cut-off (MWCO) of 350−400 Da and 2000 Da, respectively, which were provided by Ande membrane separation technology engineering Co., Ltd., China. Methyl blue (MB), as a model foulant for degradation experiments as well as fouling/cleaning experiments, was obtained from Macklin Biochemical Co., Ltd., China. Bisphenol A (BPA) for degradation experiments was obtained from Sigma-Aldrich. H_2O_2, Methanol (MeOH), and hydrochloric acid (HCl) were purchased from Sinopharm Chemical Reagent Co., Ltd., China. Glucose, sodium hydroxide, and polyethylene glycol [PEG, molecular weight (MW) of 200, 400, 600, 1000 and 1500 Da] were purchased from Xilong Scientific Co., Ltd., China. Xylose, 1, 4-benzoquinone (BQ) and dimethyl thiourea (DMTU) were purchased from Macklin Biochemical Co., Ltd., China. (3-Aminopropyl) triethoxysilane (APTES) were bought from Aladdin. *N*-(3-Dimethylaminopropyl)-*N*′-ethylcarbodiimide (EDC), *N*-hydroxy succinimide (NHS), and 2-(*N*-morpholine) ethanesulfonic acid (MES) were purchased from Beijing Chemicals Work, China. All chemicals were used without further purification. Unless otherwise specified, all solutions were prepared with deionized water.

2.2. Catalytic Performance Testing. *2.2.1. Degradation Experiments.* All degradation experiments were conducted in 100 mL beakers in a shaker (150 rpm) at room temperature (25 °C). In each beaker, a 20 mL of reaction solution was composed of MB (10 mg L^{-1}) and the oxidation system (Table 1). The initial pH value of the reaction solution was adjusted to 5.5 by HCl and NaOH. During the degradation, 1 mL of the reaction solution was sampled at predetermined intervals, followed by the filtration through 0.22 μm filter membranes. The MB concentration was determined by measuring the maximum absorption band (630 nm) using a UV−vis spectrophotometer (UV5 Bio, Mettler-Toledo, Switzerland) and calculating according to the standard curve of MB. The sample was poured back into the reaction solution after the measurement. Besides MB, BPA (5 mg L^{-1}) was also used as a substrate to examine the degradation efficiency of different oxidation systems using the same protocol. BPA concentration detection method is illustrated in the Supporting Information.

Table 1. Content and Dosage of Different Oxidation Systems

Oxidation systems	Reagents and dosage
H_2O_2	10 mM H_2O_2[a]
GOD	0.1 mg mL^{-1} GOD, 100 mM glucose[b]
H_2O_2−Fe_3O_4	10 mM Fe_3O_4, 10 mM H_2O_2
GOD−Fe_3O_4	10 mM Fe_3O_4, 0.1 mg mL^{-1} GOD, 100 mM glucose

[a]The dosage was similar to the amount of H_2O_2 produced in the GOD enzymatic reaction. [b]Glucose acted as the substrate in the GOD enzymatic reaction to generate H_2O_2.

2.2.2. Effect of pH. In this section, the degradation experiments were carried out in deionized water and acetate buffer solution (to maintain the pH value constant) with an initial pH of 5.5, respectively. The solution pH was monitored throughout the duration of the degradation experiments using a pH meter.

2.2.3. Quenching Experiments. Quenching experiments were performed by adding the desired scavengers into the reaction solution before the addition of GOD−Fe_3O_4 and MB. Three scavengers, MeOH, 1,4-BQ, and DMTU, were used for quenching OH·, O^{2-}·, and H_2O_2, respectively.

2.3. Membrane Fouling/Cleaning Experiments. To examine the capability of the catalyst on membrane fouling removal, the flux variation of the NF10 membrane in fouling/cleaning experiments was studied. MB was chosen as the model foulant due to its good solubility and ubiquity in wastewater. A dead-end filtration cell (Amicon 8050, Millipore, U.S.A.) with an effective area of 13.4 cm^2 was used to filter the MB solution (20 mg L^{-1}, pH = 5.5) by the NF10 membrane. The fouling experiment was carried out by filtration of MB solution at 1 bar (150 rpm, 25 °C) for 1 h, and the flux was recorded every 15 min. After filtration, the retentate was poured out, and the membrane was rinsed using deionized water to remove the weakly attached foulants. The water flux of the fouled membrane was measured at 1 bar for three times. Then, 20 mL of the oxidation system (Table 1) or deionized water was used as cleaning agents and

https://doi.org/10.1021/acsami.1c23466
ACS Appl. Mater. Interfaces XXXX, XXX, XXX−XXX

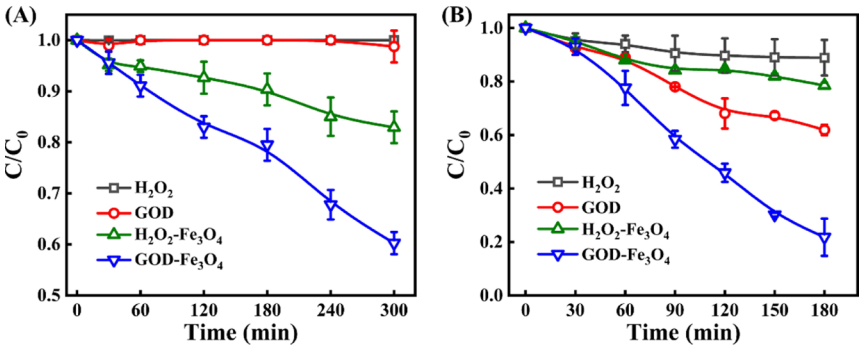

Figure 1. Degradation efficiency of (A) BPA and (B) MB by different oxidation systems.

added to the cell (pH = 5.5), and the cell was placed in a shaker (150 rpm, 25 °C) for 30 min to perform membrane cleaning. After that, the cleaning agent was removed, and the membrane was rinsed using deionized water to remove residual agents. The water flux of the cleaned membrane was also measured for three times. Fouling/cleaning experiments were conducted using the same protocol for three cycles to evaluate the cleaning efficiency of different cleaning agents. The membranes were thoroughly rinsed with deionized water before each solution replacement. In addition, zeta potential, contact angle, and FITR analysis were used to evaluate the change of membrane surface properties before and after fouling/cleaning.

2.3.1. Calculation. Permeate flux (J) was calculated as eq 3.

$$J = \frac{V_p}{t \times A_m} \tag{3}$$

where V_p is the permeate volume after t time; A_m is the effective membrane area.

The flux variation of the membrane was reflected by normalized flux according to eq 4.

$$\text{Normalized flux} = \frac{J}{J_0} \tag{4}$$

where J and J_0 are the recorded flux and the initial water flux of membranes, respectively.

The flux recovery rate (FRR) was calculated to assess the cleaning efficiency of the catalyst system by eq 5.

$$\text{FRR}\ (\%) = \frac{J_c}{J_o} \times 100 \tag{5}$$

where J_c is the water flux of the cleaned membrane.

2.4. Effect of Catalysis Reactions on the Polyamide NF Membrane. *2.4.1. Long-Term Treatment.* To assess the influence of catalysis reactions on the membrane, the NF10 membrane was treated with GOD−Fe_3O_4 and H_2O_2−Fe_3O_4 catalyst systems for 12 h, respectively. Specifically, the membrane was placed in a dead-end filtration cell with the separation layer facing up and was treated by 20 mL reaction solution with shaking (25 °C and 150 rpm) for 12 h. By measuring the water flux and pore size distribution of the membrane before and after the long-term treatment, the effect of two catalysis reactions on membrane separation performances and surface properties was examined. Besides the NF10 membrane, the homogeneous NF5 membrane with smaller pore size (MWCO: 350−400 Da) was also conducted to reveal the effect of two catalysis reactions on a polyamide NF membrane with different pore size. All the other experimental procedures were the same as those of the NF10 membrane.

2.4.2. Determination of Membrane Pore Size Distribution. Pore size distribution of NF10 and NF5 membranes before and after catalytic treatment was determined, respectively, by separation of neutral solutes. According to the estimated pore size of the membranes, xylose and PEG (MW of 200, 400, 600, 1000, and 1500 Da) were chosen as the molecular probes in this study. Typically, a dead-end filtration setup was used to filter 0.2 g L^{-1} of the molecular probe solution in the order of MW from smallest to largest. The filtration conditions were as follows: 1 bar, 150 rpm, and room temperature (25 °C). Total volume of solution added into the cell was 30 mL, and the filtration was stopped when 10 mL of the permeate solution was collected. The molecular probe concentration of feed and permeate solution was determined using total organic carbon (TOC, Shimadzu, Japan). The rejection (R) for xylose/PEG molecules was calculated by the following equation

$$R\ (\%) = \left(1 - \frac{C_p}{C_f}\right) \times 100 \tag{6}$$

where C_f and C_p are xylose/PEG concentrations of feed and permeate solution, respectively.

Without considering influences of the steric and hydrodynamic interaction between solute and membrane pores, the pore size distribution of the membranes can be expressed through the following probability density function

$$\frac{dR(d_p)}{dd_p} = \frac{1}{\sqrt{2\pi}\, d_p \ln \sigma_p} \exp\left[-\frac{(\ln d_p - \ln \mu_p)^2}{2(\ln \sigma_p)^2}\right] \tag{7}$$

where d_p represents the solute Stokes diameter; μ_p is the mean effective pore size, which is determined at solute rejection R = 50%; σ_p refers to the geometric standard deviation, which is defined as the ratio of d_p at R = 84.13% over that at R = 50%.

2.5. Preparation of the Reusable Catalyst for Membrane Cleaning. To further save cleaning costs, the reusable catalysts were prepared by amination modification and subsequent GOD immobilization on Fe_3O_4. Specifically, 50 mg of Fe_3O_4 nanoparticles was added into 80 mL of the ethanol−water mixed solvent ($V_{ethanol}$:V_{water} = 1:1) to form stable disperse solution under ultrasonication for 1 h. Then, 2 mL of APTES was added to the above solution, and the amino−functionalization reaction was carried out under stirring (400 rpm, 50 °C) for 24 h. After that, the obtained amino-functionalized Fe_3O_4 (Fe_3O_4−NH_2) nanoparticles were washed three times by fresh ethanol and deionized water. The GOD-immobilized Fe_3O_4 (GOD@Fe_3O_4) magnetic nanoparticles were prepared by adding the as-prepared Fe_3O_4−NH_2, 2 mg of GOD, and 20 mL of the activation solution in a 50 mL centrifuge tube and shaking (150 rpm, 25 °C) for 3 h. The activation solution, aiming to facilitate the interaction between the carboxyl group on GOD and the amino group on Fe_3O_4−NH_2, was prepared by 15.6 mg of EDC and 9.4 mg NHS with 20 mL MES buffer (0.1 M, pH = 5.0). The GOD@Fe_3O_4 nanoparticles were separated under a magnetic field and washed several times using fresh deionized water to remove the weakly combined GOD. Finally, GOD@Fe_3O_4 nanoparticles were dispersed in 20 mL of deionized water for pollutant degradation/membrane cleaning experiment.

The pollutant degradation (MB and real molasses fermentation wastewater) and the fouling/cleaning experiment using GOD@Fe_3O_4 nanoparticles was conducted with the same protocol in Sections 2.2 and 2.3 for several cycles. After each catalytic degradation/cleaning

https://doi.org/10.1021/acsami.1c23466
ACS Appl. Mater. Interfaces XXXX, XXX, XXX−XXX

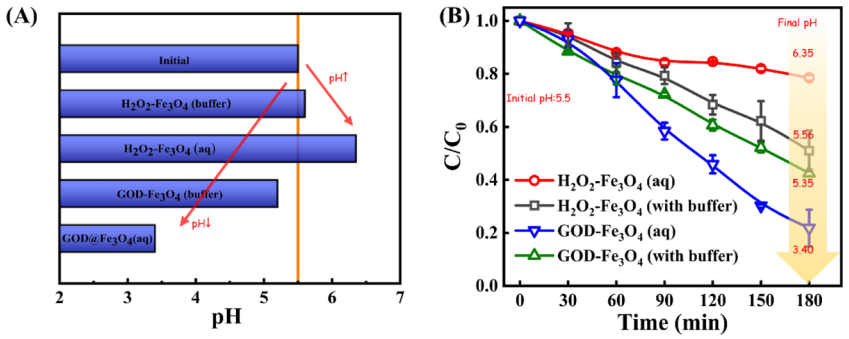

Figure 2. (A) pH change of different oxidation systems after 180 min reaction. (B) MB degradation efficiency of GOD−Fe_3O_4 and H_2O_2−Fe_3O_4 in deionized water and acetic acid buffer solution, respectively.

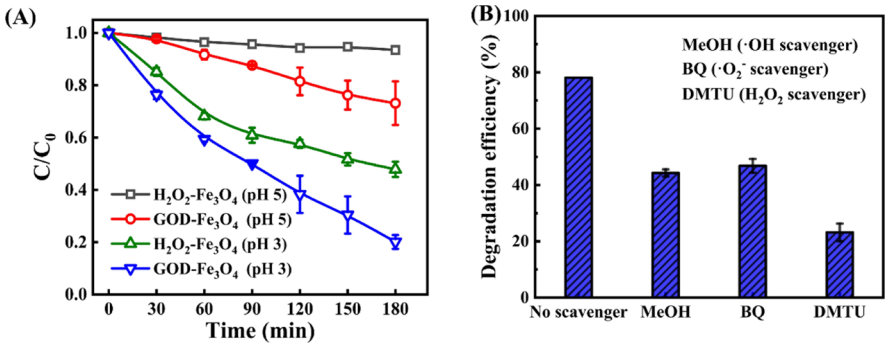

Figure 3. (A) MB degradation efficiency by GOD−Fe_3O_4 and H_2O_2−Fe_3O_4 systems at pH 3 and pH 5, respectively. (B) Effects of different scavengers on MB degradation efficiency by the GOD−Fe_3O_4 system (MB concentration: 25 mg L^{-1}).

step, GOD@Fe_3O_4 nanoparticles were recycled and completely rinsed using deionized water under a magnetic field, and the fresh glucose solution was added for a new round of catalysis/cleaning.

3. RESULTS AND DISCUSSION

3.1. Construction of the Chemoenzymatic Cascade Catalysis System. *3.1.1. Removal of Phenolic Derivatives and Dye Pollutants.* We first compared the oxidizing capability of pollutants by different oxidation systems. Here, BPA and MB were selected as model pollutants because of their small MW, which are more likely to cause membrane fouling in the NF process. To maximize the synergistic effect of two catalysis in the cascade process, the optimal ratio of the catalysts ($m_{Fe_3O_4}$:m_{GOD} ratio of 23) was determined in terms of reactant consumption, catalytic activity as well as reaction kinetics (as shown in Figures S1 and S2), and this ratio was adopted in the whole experiment. From the result exhibited in Figure 1, we found that BPA concentration barely changed in the single H_2O_2 or single GOD system, revealing that H_2O_2 and GOD catalysis cannot effectively decompose pollutants without activation by other catalysts.[20] The effective degradation of BPA occurred in the presence of the Fe_3O_4 catalyst since reactive free radicals were generated during the Fenton process and exhibited strong oxidizing activity for organic pollutant degradation. In the chemoenzymatic cascade system (GOD−Fe_3O_4) with H_2O_2 as the intermediate product, the degradation efficiency of BPA was about 39.8% after 300 min, which is significantly higher than that of the traditional Fenton system (H_2O_2−Fe_3O_4, 17.1%). Similar results could be found in the MB degradation experiment, in which 78.3% within 180 min could be achieved in the GOD−Fe_3O_4 system, while only 11.1% in the H_2O_2−Fe_3O_4 system (Figure 1B). This can be explained by the different production ways of H_2O_2; that is, H_2O_2 was gradually generated in the GOD−Fe_3O_4 system, while that was one-time addition in the H_2O_2−Fe_3O_4 system and excessive H_2O_2 could trigger substrate inhibition.[21] Moreover, the pH adjustment mechanism in the GOD−Fe_3O_4 system is the other reason for its high degradation efficiency, since the GOD catalytic reaction can produce D-gluconic acid and thus reduce the pH of the system, and the catalytic activity of Fe_3O_4 is higher in the acidic condition (as shown in Figure S3).[18] It is worth noting that MB degradation efficiency in the single GOD system was higher than that in the single H_2O_2 system, which can be ascribed to the adsorption of part MB molecules on enzymes.

3.1.2. Microenvironment pH Adjustment Mechanism. To further verify the pH adjustment mechanism in the chemoenzymatic reaction system, we conducted GOD−Fe_3O_4 and H_2O_2−Fe_3O_4 reaction in deionized water and acetic acid buffer, respectively. The initial pH was adjusted to 5.5 using HCl, and the buffer solution was used to maintain the pH value throughout the reaction (pH 5.5 was determined by the GOD reaction to properly initiate the cascade reaction, as shown in Figure S3). The result showed the pH value of the GOD−Fe_3O_4 system after 180 min reaction decreased significantly from initial 5.5 to 3.4 (Figure 2A), which was attributed to the production of D-gluconic acid through enzymatic catalysis. It is well known that the acidic environment is favorable for a stable circulation of Fe^{2+}/Fe^{3+} on the Fe_3O_4 surface, which can not only accelerate the reaction rate but also avoid the deposition of ferric hydroxide.[22] Therefore, the MB degradation efficiency by the GOD−Fe_3O_4 system in deionized water reached up to 78.3%, which is notably higher than that in buffer solution (Figure 2B). On the contrary, for the H_2O_2−Fe_3O_4 system, the MB degradation efficiency in deionized water (11.1%) was lower

https://doi.org/10.1021/acsami.1c23466
ACS Appl. Mater. Interfaces XXXX, XXX, XXX−XXX

than that in buffer solution (49.0%). It is because the pH value increased from 5.5 to 6.35 in the deionized water as the reaction progresses, and the catalytic activity of Fe_3O_4 would reduce as pH increased, as shown in Figure S3. In this work, the cascade reaction exhibited outstanding pH adjustment ability without additional chemical reagents, which is considered to be one of the advanced features of the chemoenzymatic cascade reaction compared to the traditional Fenton reaction.

3.1.3. Catalytic Process and Mechanism Exploration. It was verified that the acidic condition contributed to the rapid degradation of pollutants, then, if there is still a superiority of the chemoenzymatic cascade reaction when the pH was directly adjusted to a strong acidic condition? We first explored the pH evolution in the different oxidation systems with an initial pH at 3, and the result exhibited that the pH variation of both H_2O_2−Fe_3O_4 and GOD−Fe_3O_4 systems is negligible (Figure S4). However, the GOD−Fe_3O_4 system still showed higher MB degradation efficiency (80.0%) than the H_2O_2−Fe_3O_4 system (52.1%) (Figure 3A). As mentioned in Section 3.1.1, positively charged GOD (isoelectric point is 4.2) in pH 3 condition can adsorb part of the negatively charged MB molecules. We thereby investigated the adsorption capability of GOD to MB. As shown in Figure S5, nearly 20% of MB was adsorbed on GOD after adsorption−desorption equilibration at pH 3, which is consistent with the enhanced degradation efficiency in the GOD−Fe_3O_4 system. Such an adsorption effect of GOD can also promote the mass transfer of the substrate in the reaction system and improve the accessibility of the pollutant to catalysts, accelerating the process of oxidative degradation.[23]

It is reported that the degradation of pollutants is generally caused by free radicals, and OH· has been recognized as the dominant one in the Fenton reaction. To further explore the contributing free radicals in the chemoenzymatic cascade reaction and clarify its degradation mechanism, radical quenching experiments were carried out, and three radical quenchers, MeOH, 1,4-BQ, and DMTU, were selected to quench OH·, O^{2-}·, and H_2O_2, respectively. As shown in Figure 3B, the addition of MeOH significantly reduced the degradation efficiency of MB by GOD−Fe_3O_4 (46.8%), indicating that OH· can effectively destroy the chromogenic functional groups of MB molecules. Moreover, after the addition of 1,4-BQ, the degradation efficiency exhibited 44.2% decrease, which indicates that O^{2-}· also played a vital role in pollutant decomposition in the chemoenzymatic cascade reaction. We found the quenching of H_2O_2 also reduced the MB degradation efficiency of GOD−Fe_3O_4 (23.2%), a possible reason of which is the less H_2O_2 hindering the formation of OH· and O^{2-}· (H_2O_2 cannot directly induce the degradation of MB as proved in Figure 1B). Therefore, OH·, O^{2-}·, and H_2O_2 were proved to be the predominant active species to the pollutant degradation in the chemoenzymatic cascade reaction, and the possible degradation mechanism is described as the following process (Figure 4)[24]

$$\text{glucose} + O_2 \xrightarrow{\text{GOD}} \text{D} - \text{gluconic acid} + H_2O_2 \quad (8)$$

$$Fe^{2+} + H_2O_2 \rightarrow Fe^{3+} + OH\cdot \quad (9)$$

$$Fe^{3+} + H_2O_2 \rightarrow Fe^{2+} + OH_2\cdot \quad (10)$$

$$Fe^{2+} + O_2 \rightarrow Fe^{3+} + O^{2-}\cdot \quad (11)$$

$$Fe^{2+} + O^{2-}\cdot + 2H^+ \rightarrow Fe^{3+} + H_2O_2 \quad (12)$$

$$OH_2\cdot \leftrightarrow O^{2-}\cdot + H^+ \quad (13)$$

$$OH\cdot/O^{2-}\cdot + R \rightarrow \text{by} - \text{products} \quad (14)$$

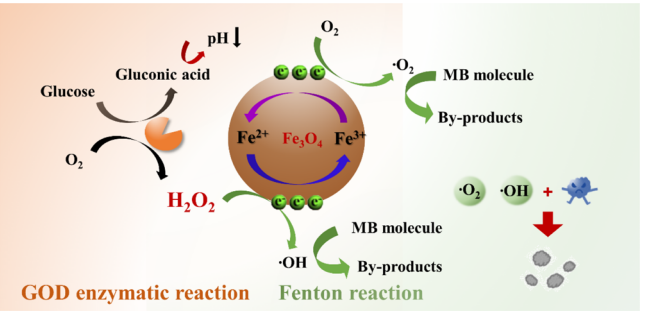

Figure 4. Degradation mechanism in the chemoenzymatic cascade reaction.

3.2. Membrane Cleaning Behavior Exploration.

3.2.1. Effect of Cleaning Agents on Flux Recovery. To evaluate the applicability of the chemoenzymatic cascade system on membrane cleaning, we designed a 3-cycle fouling/cleaning experiment and compared the cleaning efficiency of different agents. The original water flux, the water flux after fouling, and the recovered flux after cleaning were recorded, and the normalized flux of the membrane under various conditions acted as an indicator of membrane performance. From Figure 5A, we observed that water flux after fouling was lower than the MB flux at the end of the fouling process, possibly because the MB fouling layer was compacted during the subsequent water filtration process. When the fouled membrane was cleaned by different cleaning agents, it was noticed that the water flux of the membrane restored in some extent in all situations. By the comparison of water flux recovery after cleaning by different agents, we found GOD−Fe_3O_4 had a remarkable effect and its FRR reached up to 100% in the first cycle, while the FRRs for single GOD cleaning, single H_2O_2 cleaning, H_2O_2−Fe_3O_4 cleaning, and water cleaning were only 89, 84, 82, and 81%, respectively (Figure 5B). The GOD-Fe_3O_4 agent showed good reusability, whose FRR exhibited only 5% decline after 3 reuse cycles, while the others displayed obvious decline in cleaning efficiency.

To confirm that the flux recovery was not achieved at the expense of membrane damage, a series of characterizations were performed to demonstrate the membrane surface properties after fouling and cleaning (Figure S6). For the FTIR result, the new peak at 1036 cm^{-1} was attributed to the sulfonic acid group and indicated the formation of the MB fouling layer, and its diminution after cleaning represented the removal of MB molecules. The zeta potential and contact angle of the fouled membrane increased obviously compared to the pristine membrane due to the weaker negative charge and high roughness of the MB fouling layer and partially restored to the initial values after the cleaning operation. It should be noted that the zeta potential and contact angle of the membrane decreased significantly after exposure to H_2O_2, possibly ascribed to the increased hydroxyl groups on the membrane surface resulting from membrane hydrolysis.[25] In the chemoenzymatic cascade reaction, since H_2O_2 is the intermediate that can be instantly oxidized to free radicals, the accumulation of

https://doi.org/10.1021/acsami.1c23466
ACS Appl. Mater. Interfaces XXXX, XXX, XXX−XXX

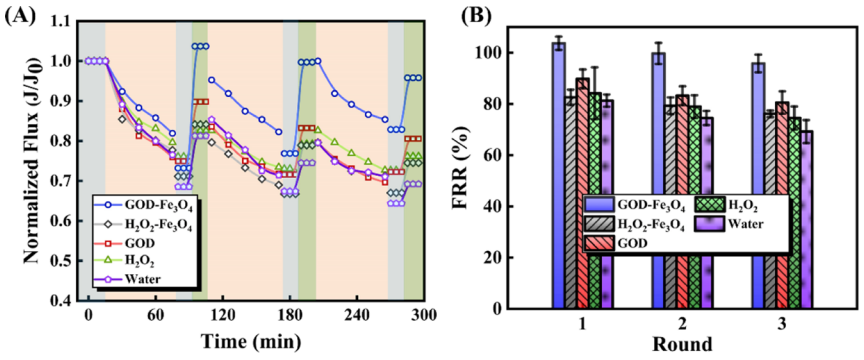

Figure 5. (A) Flux variation in the fouling/cleaning experiment. (B) Flux recovery rate of the membrane cleaned by various oxidation systems. (The blue areas represent water flux; the green areas represent water flux after cleaning; and the yellow areas represent the flux of MB filtration).

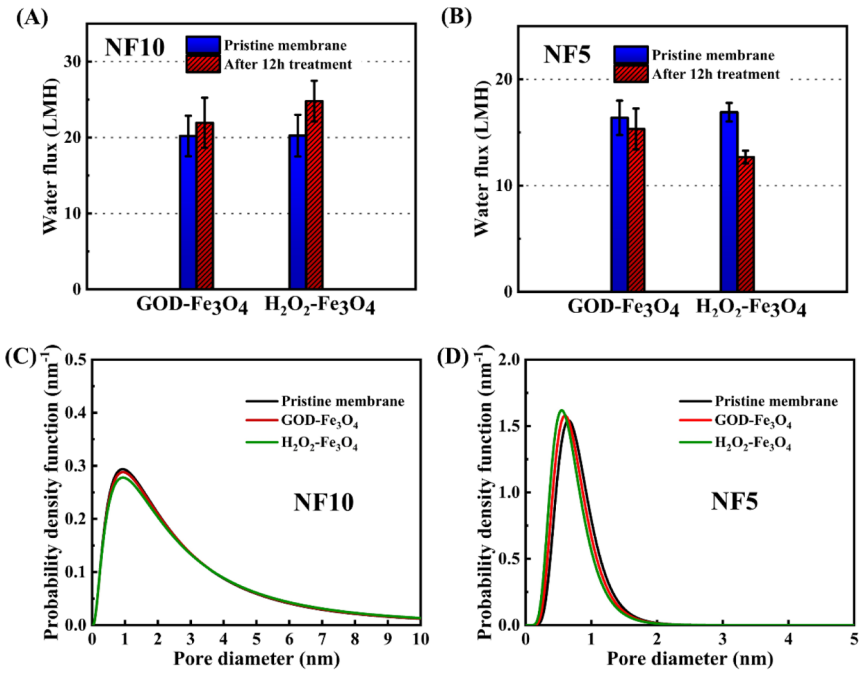

Figure 6. Permeability and pore size distribution of the (A,C) NF10 membrane and (B,D) NF5 membrane before and after catalysis reactions for 12 h, respectively.

H_2O_2 would be prevented to lower the risk of membrane damage.

3.2.2. Effect of Catalysis Reactions on the Polyamide NF Membrane. Traditional Fenton reaction would oxidize the polyamide structure by the formed massive free radicals and thus damage the membrane.[26,27] To evaluate the tolerance of the polyamide NF membrane to the chemoenzymatic cascade reaction, the separating layer of the membrane was exposed to the GOD−Fe_3O_4 agent for 12 h, and the water flux before and after treatment was measured as the indicator of membrane performance. A control experiment was conducted using the H_2O_2−Fe_3O_4 agent. Moreover, a homogeneous NF5 membrane with smaller pore size (MWCO: 350−400 Da) was also used to reveal the effect of the chemoenzymatic cascade reaction on the polyamide NF membrane with different pore sizes. As seen in Figure 6A, the water flux of the NF10 membrane gained less increase after being exposed to GOD−Fe_3O_4 (~8.6%) than H_2O_2−Fe_3O_4 (~22.4%) for 12 h. This indicates that the tolerance of the NF10 membrane in the cascade reaction was higher than that in the traditional Fenton reaction. Contrary to the NF10 membrane, the water flux of the NF5 membrane decreased significantly after both long-term treatments. Considering that the separation layer of the NF5 membrane is denser, this result is probably caused by ferric hydroxide precipitation blocking the membrane pores. Although the flux changes of these two different polyamide NF membranes after treatments exhibited opposite trends, both of them had stronger resistance in the chemoenzymatic cascade reaction.

To further explore the effect mechanism of traditional Fenton reaction and chemoenzymatic cascade reaction on polyamide NF membranes with different pore sizes, we investigated the pore sizes and their distribution of the membranes, which were calculated from the solute rejection of neutral hydrophilic molecules with the help of the mathematical modeling. From Figure 6C and Table 2, it is found that the NF10 membrane has a slightly greater pore size (μ_p = 2.288 and 2.362 for GOD-Fe_3O_4- and H_2O_2−Fe_3O_4-treated membranes, respectively) and a wider pore size distribution (σ_p = 2.571 and 2.620 for GOD−Fe_3O_4- and H_2O_2−Fe_3O_4-treated membranes, respectively) after treatment than the pristine membrane (μ_p = 2.242, σ_p = 2.559). On the

https://doi.org/10.1021/acsami.1c23466
ACS Appl. Mater. Interfaces XXXX, XXX, XXX−XXX

Table 2. Mean Effective Pore Size (μ_p) and Geometric Standard Deviation (σ_p) of NF10 and NF5 Membranes before and after Catalysis Reactions

	NF10		NF5	
	μ_p (nm)	σ_p	μ_p (nm)	σ_p
pristine	2.242	2.559	0.748	1.448
GOD−Fe_3O_4	2.288	2.571	0.696	1.478
H_2O_2−Fe_3O_4	2.362	2.620	0.651	1.511

basis of above results, we attributed the flux increase of the NF10 membrane after both reactions to the oxidation of the amide structure and loosening of the membrane cross-linking in some regions. Thanks to the in situ production and prompt consumption of H_2O_2 in the chemoenzymatic cascade reaction, less hydrolysis occurred on the membrane surface, thus resulting in fewer changes on pore size/pore size distribution. Moreover, the pH adjustment mechanism in the chemoenzymatic cascade reaction can maintain an acidic microenvironment for the system, effectively preventing the self-decomposing of H_2O_2 under alkaline conditions to form free radicals, which would attack the membrane materials. As for the NF5 membrane, the mean effective pore size decreased and the pore size distribution increased, confirming the blockage of some small membrane pores by ferric hydroxide precipitation (Figure 6D). It is reported that biological macromolecules rich in carboxyl and hydroxyl groups can reduce the release of ferric hydroxide precipitation via the chelation effect. Therefore, the less influence of the GOD−Fe_3O_4 reaction on the water flux and membrane pores is probably due to the existence of GOD molecules.

3.3. Reuse of Chemoenzymatic Catalysts for Membrane Cleaning. To improve the economy and sustainability of the chemoenzymatic cascade reaction in membrane cleaning, we designed a reusable cascade catalyst by amination modification followed by GOD immobilization on Fe_3O_4 magnetic nanoparticles (as shown in Figure 7A).[28] FTIR spectra of Fe_3O_4, Fe_3O_4−NH_2, and GOD@Fe_3O_4 nano-

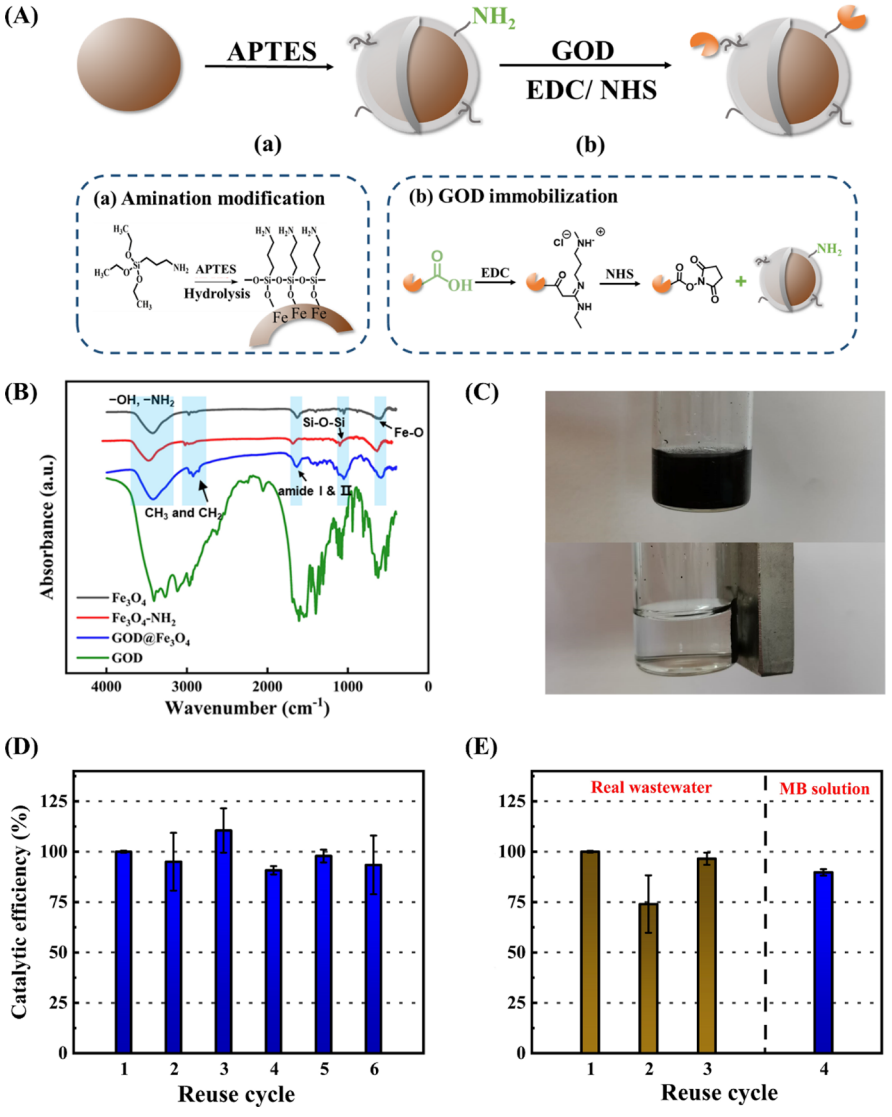

Figure 7. (A) Modification strategy of the reusable cascade catalysts. (B) FTIR spectra of Fe_3O_4, Fe_3O_4−NH_2, and GOD@Fe_3O_4 nanoparticles and GOD enzyme molecules. (C) Recovery of GOD@Fe_3O_4 nanoparticles under a magnetic field. (D) Catalytic efficiency of GOD@Fe_3O_4 nanoparticles on methyl blue (MB) degradation with a reuse cycle. (E) Catalytic efficiency of GOD@Fe_3O_4 nanoparticles on cane molasses wastewater decolorization with a reuse cycle [the fourth cycle was carried out for MB degradation compared to the result in (D)].

https://doi.org/10.1021/acsami.1c23466
ACS Appl. Mater. Interfaces XXXX, XXX, XXX−XXX

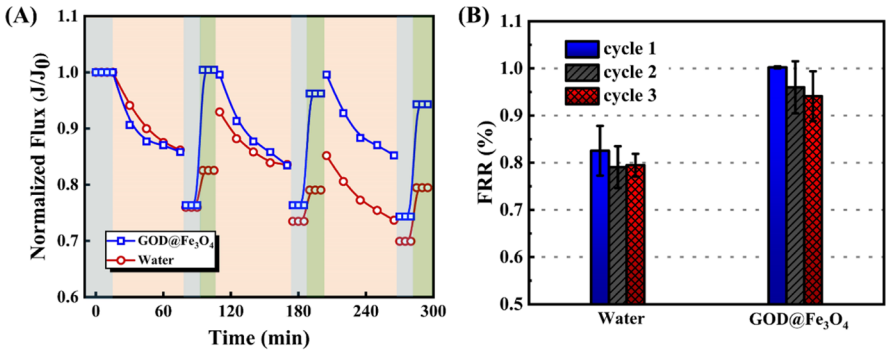

Figure 8. (A) Flux variation in the fouling/cleaning experiment using water and GOD@Fe_3O_4 as the reagents, respectively. (B) Flux recovery rate of the membrane cleaned by water and GOD@Fe_3O_4 reagent, respectively.

particles and GOD enzyme molecules respectively were carried out to verify the successful modification. As seen in Figure 7B, the FTIR results around 587 cm^{-1} for three kinds of nanoparticles are ascribed to the Fe−O stretching vibration in Fe_3O_4. For the Fe_3O_4−NH_2 nanoparticles, the new peak at 1094 cm^{-1} is attributed to the Si−O−Si group of ATPES alkoxysilane molecules, indicating the successful ATPES amination modification, which is also consistent with the result in EDX analysis (the noticeable Si signal in Figure S7).[29] The peaks at 3485 and 1690 cm^{-1} are ascribed to the N−H stretching vibration and NH_2 stretching, respectively, and its difference with Fe_3O_4 also implicates the successful fabrication of Fe_3O_4−NH_2 nanoparticles.[30] It is noted that some characteristic peaks of the free GOD enzyme are generated by the C−H bond in CH_3 and CH_2 groups, Amide A, C═O bond of amide I, and N−H bond of amide II.[31] Therefore, for the results of GOD@Fe_3O_4 nanoparticles, the new peaks at 2855 and 2930 cm^{-1} are derived from C−H stretching vibration of CH_3 and CH_2 groups, which illustrates the presence of GOD. The increase in the broad peak at 3000 to 3700 cm^{-1} is ascribed to the Amide A band, and the increase on the peak of 1500 to 1700 cm^{-1} is attributed to C═O stretching amide I and N−H bending amide II. Moreover, although the nanoparticles morphology does not significantly change after modification and enzyme immobilization in SEM images (Figure S7A−C), their elements distribution variations based on EDX results (Figure. S7D−F) verify the above discussions. All these results show that GOD enzyme molecules have been successfully immobilized on the Fe_3O_4 nanoparticles.

From Figure 7C, we can observe that GOD@Fe_3O_4 catalysts are able to be conveniently retrieved under an external magnetic, which is conducive to the sustainability of the membrane cleaning strategy. The MB model solution and real molasses wastewater were respectively applied to evaluate the catalytic stability of the GOD@Fe_3O_4 nanoparticles during reuse. As shown in Figure 7D, a stable catalytic efficiency in the degradation of MB (>90%) within 6 reuse cycles implies negligible loss of catalyst activity of the GOD@Fe_3O_4 nanoparticles during the reuse and magnetic recovery processes. Similar results can be found in the treatment of real molasses wastewater, and its complex components (e.g., Mg^{2+}) may affect the Fenton reaction rate but would not inactivate GOD@Fe_3O_4,[32] which is confirmed by a high catalytic efficiency in the following MB degradation (Figure 7E). Meanwhile, compared to the free GOD−Fe_3O_4 system, the glucose consumption of the GOD@Fe_3O_4 system can be reduced by 50% (Figure S8), which is favorable for the cost saving of this green cleaning method.

Furthermore, we investigated the reusability of GOD@Fe_3O_4 nanoparticles on membrane cleaning, and the fouling/cleaning experiment was conducted using the same protocol. As shown in Figure 8A, the membrane performance can be almost completely restored after cleaning by GOD@Fe_3O_4 nanoparticles in each cycle, and the flux recovery rate still reached up to 94% after three cycles (Figure 8B). This result demonstrates that the cleaning effect of the recycled GOD@Fe_3O_4 nanoparticles is not inferior to the free cascade catalysts (GOD−Fe_3O_4) in the cleaning of polyamide NF membranes. In addition, the economic evaluation shows that the GOD@Fe_3O_4 cleaning method costs around 16.5 times less than that using the commercial chemical cleaning agent (e.g., Ultrasil 110), indicating its low-cost and great potential in the real applications (Supporting Information). Therefore, the reusable GOD@Fe_3O_4 magnetic nanoparticles with a stable catalytic efficiency and an outstanding cleaning effect provides a green and cost-effective approach for multi-cycle membrane cleaning.

4. CONCLUSIONS

In conclusion, a chemoenzymatic cascade reaction consisting of GOD and Fe_3O_4 is proposed for pollutant degradation and polyamide NF membrane cleaning. First, the GOD−Fe_3O_4 cascade system exhibits superior degradation efficiency on BPA and MB compared to the single enzymatic/oxidative or traditional Fenton reaction. On the one hand, the pH adjustment mechanism in the GOD−Fe_3O_4 cascade system ensures the system an acid environment for the high activity of Fenton reactions; on the other hand, the substrate enrichment of GOD molecules promotes the mass transfer and the oxidative process. Then, the GOD−Fe_3O_4 cascade system is used as the cleaning agent to regenerate the MB fouled polyamide NF membrane, and membrane performance can be almost completely recovered after cleaning. Moreover, the cascade mode, in which H_2O_2 is the intermediate, enables the in-situ production and the instant consumption of H_2O_2 and thus avoids high concentration of H_2O_2 in the system to damage membrane materials. Therefore, the polyamide NF membrane exhibits a strong tolerance to the chemoenzymatic cascade reaction. The produced iron hydroxide precipitation during the reaction can also be chelated with GOD biomolecules in the cascade system and reduce the impairment on NF membrane performance. Finally, the reusable catalysts, which can be retrieved under an external magnetic field, are prepared through amination modification and subsequent

https://doi.org/10.1021/acsami.1c23466
ACS Appl. Mater. Interfaces XXXX, XXX, XXX−XXX

GOD immobilization on Fe_3O_4 nanoparticles. The reused GOD@Fe_3O_4 nanoparticles exert favorable cleaning efficiency in three cycles of fouling removal and provide a sustainable and cost-effective approach for polyamide NF membrane cleaning.

■ ASSOCIATED CONTENT

Supporting Information

The Supporting Information is available free of charge at https://pubs.acs.org/doi/10.1021/acsami.1c23466.

Materials and methods, effect of catalysts mass ratios on glucose consumption, gluconic acid yield, and the catalytic activity, the calculation of V_{max} and K_M, effect of pH on the catalytic activity, pH evolution, adsorption of MB on three catalysts, FTIR spectra, zeta potential and contact angle of pristine, fouled and cleaned membrane, SEM images and EDX analysis of three kinds of nanoparticles, MB degradation efficiency of GOD@Fe_3O_4 under different glucose concentrations, and the economic evaluation of the GOD@Fe_3O_4 cleaning agent (PDF)

■ AUTHOR INFORMATION

Corresponding Author

Jianquan Luo − *State Key Laboratory of Biochemical Engineering, Institute of Process Engineering, Chinese Academy of Sciences, Beijing 100190, China; School of Chemical Engineering, University of Chinese Academy of Sciences, Beijing 100049, PR China;* orcid.org/0000-0002-9949-7779; Phone: +86 01082544991; Email: Jqluo@ipe.ac.cn; Fax: +86 01062650673

Authors

Jinxuan Zhang − *State Key Laboratory of Biochemical Engineering, Institute of Process Engineering, Chinese Academy of Sciences, Beijing 100190, China; School of Chemical Engineering, University of Chinese Academy of Sciences, Beijing 100049, PR China*

Huiru Zhang − *State Key Laboratory of Biochemical Engineering, Institute of Process Engineering, Chinese Academy of Sciences, Beijing 100190, China; School of Chemical Engineering, University of Chinese Academy of Sciences, Beijing 100049, PR China*

Yinhua Wan − *State Key Laboratory of Biochemical Engineering, Institute of Process Engineering, Chinese Academy of Sciences, Beijing 100190, China; Ganjiang Innovation Academy, Chinese Academy of Sciences, Ganzhou 341000, PR China*

Complete contact information is available at: https://pubs.acs.org/10.1021/acsami.1c23466

Author Contributions

‖These authors contributed equally.

Notes

The authors declare no competing financial interest.

■ ACKNOWLEDGMENTS

This work was supported by the National Natural Science Foundation of China (no. 21878306) and the Beijing Natural Science Foundation (2192053).

■ REFERENCES

(1) Zhang, H.; He, Q.; Luo, J.; Wan, Y.; Darling, S. B. Sharpening Nanofiltration: Strategies for Enhanced Membrane Selectivity. *ACS Appl. Mater. Interfaces* **2020**, *12*, 39948−39966.

(2) Guo, S.; Wan, Y.; Chen, X.; Luo, J. Loose Nanofiltration Membrane Custom-Tailored for Resource Recovery. *Chem. Eng. J.* **2021**, *409*, 127376.

(3) Li, S.; Luo, J.; Hang, X.; Zhao, S.; Wan, Y. Removal of Polycyclic Aromatic Hydrocarbons by Nanofiltration Membranes: Rejection and Fouling Mechanisms. *J. Membr. Sci.* **2019**, *582*, 264−273.

(4) Kim, S.; Chu, K. H.; Al-Hamadani, Y. A. J.; Park, C. M.; Jang, M.; Kim, D.-H.; Yu, M.; Heo, J.; Yoon, Y. Removal of Contaminants of Emerging Concern by Membranes in Water and Wastewater: A Review. *Chem. Eng. J.* **2018**, *335*, 896−914.

(5) Huang, J.; Luo, J.; Chen, X.; Feng, S.; Wan, Y. How Do Chemical Cleaning Agents Act on Polyamide Nanofiltration Membrane and Fouling Layer? *Ind. Eng. Chem. Res.* **2020**, *59*, 17653−17670.

(6) Zhao, X.; Zhang, R.; Liu, Y.; He, M.; Su, Y.; Gao, C.; Jiang, Z. Antifouling Membrane Surface Construction: Chemistry Plays a Critical Role. *J. Membr. Sci.* **2018**, *551*, 145−171.

(7) Wang, X.; Hu, T.; Wang, Z.; Li, X.; Ren, Y. Permeability Recovery of Fouled Forward Osmosis Membranes by Chemical Cleaning During a Long-Term Operation of Anaerobic Osmotic Membrane Bioreactors Treating Low-Strength Wastewater. *Water Res.* **2017**, *123*, 505−512.

(8) Huang, J.; Luo, J.; Chen, X.; Feng, S.; Wan, Y. New Insights into Effect of Alkaline Cleaning on Fouling Behavior of Polyamide Nanofiltration Membrane for Wastewater Treatment. *Sci. Total Environ.* **2021**, *780*, 146632.

(9) Do, V. T.; Tang, C. Y.; Reinhard, M.; Leckie, J. O. Degradation of Polyamide Nanofiltration and Reverse Osmosis Membranes by Hypochlorite. *Environ. Sci. Technol.* **2012**, *46*, 852−859.

(10) Li, K.; Li, S.; Su, Q.; Wen, G.; Huang, T. Effects of Hydrogen Peroxide and Sodium Hypochlorite Aging on Properties and Performance of Polyethersulfone Ultrafiltration Membrane. *Int. J. Environ. Res. Public Health* **2019**, *16*, 3972.

(11) Strugholtz, S.; Sundaramoorthy, K.; Panglisch, S.; Lerch, A.; Brügger, A.; Gimbel, R. Evaluation of the Performance of Different Chemicals for Cleaning Capillary Membranes. *Desalination* **2005**, *179*, 191−202.

(12) Zhang, H.; Zhang, J.; Luo, J.; Wan, Y. A Novel Paradigm of Photocatalytic Cleaning for Membrane Fouling Removal. *J. Membr. Sci.* **2022**, *641*, 119859.

(13) De Angelis, L.; de Cortalezzi, M. M. F. Improved Membrane Flux Recovery by Fenton-Type Reactions. *J. Membr. Sci.* **2016**, *500*, 255−264.

(14) Tang, S.; Zhang, L.; Peng, Y.; Liu, J.; Zhang, Z. Fenton Cleaning Strategy for Ceramic Membrane Fouling in Wastewater Treatment. *J. Environ. Sci.* **2019**, *85*, 189−199.

(15) Shao, D.-D.; Yang, W.-J.; Xiao, H.-F.; Wang, Z.-Y.; Zhou, C.; Cao, X.-L.; Sun, S.-P. Self-Cleaning Nanofiltration Membranes by Coordinated Regulation of Carbon Quantum Dots and Polydopamine. *ACS Appl. Mater. Interfaces* **2020**, *12*, 580−590.

(16) Yang, Y.; Wang, Q.; Aleisa, R.; Zhao, T.; Ma, S.; Zhang, G.; Yao, T.; Yin, Y. Mos2/Fes Nanocomposite Catalyst for Efficient Fenton Reaction. *ACS Appl. Mater. Interfaces* **2021**, *13*, 51829−51838.

(17) Bello, M. M.; Abdul Raman, A. A.; Asghar, A. A Review on Approaches for Addressing the Limitations of Fenton Oxidation for Recalcitrant Wastewater Treatment. *Process Saf. Environ. Prot.* **2019**, *126*, 119−140.

(18) Zhang, H.; Zhang, H.; Luo, J.; Wan, Y. Enzymatic Cascade Catalysis in a Nanofiltration Membrane: Engineering the Microenvironment by Synergism of Separation and Reaction. *ACS Appl. Mater. Interfaces* **2019**, *11*, 22419−22428.

(19) Singh, P.; Youden, B.; Yang, Y.; Chen, Y.; Carrier, A.; Cui, S.; Oakes, K.; Servos, M.; Jiang, R.; Zhang, X. Synergistic Multimodal Cancer Therapy Using Glucose Oxidase@Cus Nanocomposites. *ACS Appl. Mater. Interfaces* **2021**, *13*, 41464−41472.

(20) Ma, L.; He, H.; Zhu, R.; Zhu, J.; Mackinnon, I. D. R.; Xi, Y. Bisphenol a Degradation by a New Acidic Nano Zero-Valent Iron Diatomite Composite. *Catal. Sci. Technol.* **2016**, *6*, 6066−6075.
(21) Rudroff, F.; Mihovilovic, M. D.; Gröger, H.; Snajdrova, R.; Iding, H.; Bornscheuer, U. T. Opportunities and Challenges for Combining Chemo- and Biocatalysis. *Nat. Catal.* **2018**, *1*, 12−22.
(22) Yan, Q.; Lian, C.; Huang, K.; Liang, L.; Yu, H.; Yin, P.; Zhang, J.; Xing, M. Constructing an Acidic Microenvironment by Mos2 in Heterogeneous Fenton Reaction for Pollutant Control. *Angew. Chem., Int. Ed.* **2021**, *60*, 17155−17163.
(23) Shojaat, R.; Saadatjoo, N.; Karimi, A.; Aber, S. Simultaneous Adsorption−Degradation of Organic Dyes Using Mnfe2o4/Calcium Alginate Nano-Composites Coupled with Gox and Laccase. *J. Environ. Chem. Eng.* **2016**, *4*, 1722−1730.
(24) Yan, J.; Peng, J.; Lai, L.; Ji, F.; Zhang, Y.; Lai, B.; Chen, Q.; Yao, G.; Chen, X.; Song, L. Activation Cufe2o4 by Hydroxylamine for Oxidation of Antibiotic Sulfamethoxazole. *Environ. Sci. Technol.* **2018**, *52*, 14302−14310.
(25) Weydemeyer, E. J.; Sawdon, A. J.; Peng, C.-A. Controlled Cutting and Hydroxyl Functionalization of Carbon Nanotubes through Autoclaving and Sonication in Hydrogen Peroxide. *Chem. Commun.* **2015**, *51*, 5939−5942.
(26) Ouali, S.; Loulergue, P.; Biard, P.-F.; Nasrallah, N.; Szymczyk, A. Ozone Compatibility with Polymer Nanofiltration Membranes. *J. Membr. Sci.* **2021**, *618*, 118656.
(27) Yu, L.; Ling, R.; Chen, J. P.; Reinhard, M. Quantitative Assessment of the Iron-Catalyzed Degradation of a Polyamide Nanofiltration Membrane by Hydrogen Peroxide. *J. Membr. Sci.* **2019**, *588*, 117154.
(28) Garcia, J.; Zhang, Y.; Taylor, H.; Cespedes, O.; Webb, M. E.; Zhou, D. Multilayer Enzyme-Coupled Magnetic Nanoparticles as Efficient, Reusable Biocatalysts and Biosensors. *Nanoscale* **2011**, *3*, 3721−3730.
(29) Zhang, J.; Zhou, F.; Li, S.; Wan, Y.; Luo, J. Surface Functionalization of Nanofiltration Membrane by Catechol-Amine Codeposition for Enhancing Antifouling Performance. *J. Membr. Sci.* **2021**, *635*, 119451.
(30) Fang, X.; Wang, S.; Li, Y.; Liu, X.; Li, X.; Lin, S.; Cui, Z.-K.; Zhuang, Q. Nh2-Functionalized Carbon-Coated Fe3o4 Core−Shell Nanoparticles for in Situ Preparation of Robust Polyimide Composite Films with High Dielectric Constant, Low Dielectric Loss, and High Breakdown Strength. *RSC Adv.* **2016**, *6*, 107533−107541.
(31) Portaccio, M.; Della Ventura, B.; Mita, D. G.; Manolova, N.; Stoilova, O.; Rashkov, I.; Lepore, M. Ft-Ir Microscopy Characterization of Sol−Gel Layers Prior and after Glucose Oxidase Immobilization for Biosensing Applications. *J. Sol-Gel Sci. Technol.* **2011**, *57*, 204−211.
(32) Vitale, A. A.; Bernatene, E. A.; Vitale, M. G.; Pomilio, A. B. New Insights of the Fenton Reaction Using Glycerol as the Experimental Model. Effect of O2, Inhibition by Mg2+, and Oxidation State of Fe. *J. Phys. Chem. A* **2016**, *120*, 5435−5445.

https://doi.org/10.1021/acsami.1c23466
ACS Appl. Mater. Interfaces XXXX, XXX, XXX−XXX